

Spontaneous Exfoliation of Graphene into Ionic Liquid Solution

Aaron Elbourne,¹ Ben McLean,¹ Kislun Voitchovsky,² Gregory G. Warr,³ and Rob Atkin^{1,*}

¹ The University of Newcastle Priority Research Centre for Advanced Fluids and Interfaces, Newcastle Institute for Energy & Resources (Building C), University of Newcastle, Callaghan, NSW 2308, Australia.

² Department of Physics, Durham University, Durham, England, United Kingdom.

³ School of Chemistry, The University of Sydney, NSW 2006, Australia.

*Corresponding author

All reported methods of graphene exfoliation require energy input, most commonly from sonication,¹ shaking,² or stirring.³ The reverse process – aggregation of single or few layer graphene sheets – occurs spontaneously in most solvents. This makes producing, and especially storing, graphene in economic quantities challenging,^{4,5} which is a significant barrier to widespread commercialisation. Here we show that the ionic liquids (ILs) can spontaneously exfoliate graphene from graphite at room temperature. The process is thermally activated and follows an Arrhenius-type behaviour, resulting in thermodynamically stable IL / graphene suspensions. Using atomic force microscopy, the kinetics of the exfoliation could be followed *in situ* and with sub-nanometre resolution, showing that both the size and the charge of the constituent IL ions play a key role. Our results provide a general molecular mechanism underpinning spontaneous graphene exfoliation at room temperature in electrically conducting ILs, paving the way for their adoption in graphene-based technology.

Currently, graphene is typically produced via two approaches. Bottom-up methods fabricate graphene from organic precursors via chemical vapour deposition, organic synthesis, or catalysed substrate growth, but the graphene produced has variable quality and limited sheet

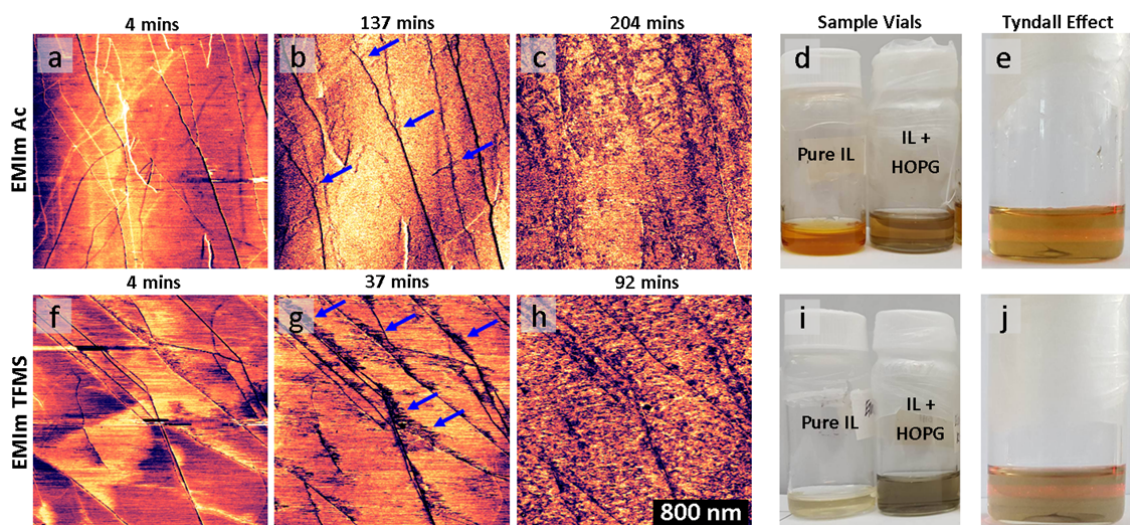
26 sizes.⁵⁻⁷ Top-down approaches exfoliate sheets from graphitic materials such as highly
27 ordered pyrolytic graphite (HOPG), carbon nanotubes, graphite intercalation compounds, and
28 graphite powders into a liquid or solution.^{5,8} While “spontaneous” graphene exfoliation has
29 previously been reported,³ in all cases samples were shaken² or stirred³ for at least 24 h,
30 meaning substantial energy was input to the system and the processes are, by definition, not
31 necessarily spontaneous.

32 Mechanical exfoliation consistently produces high-quality graphene sheets but scalability is
33 an issue, largely due to instability of the resultant graphene suspensions to aggregation.
34 Therefore exfoliation into water is performed in the presence of surfactants or polymers that
35 adsorb to the graphene surface which impede, but do not eliminate, aggregation. More stable
36 suspensions result when graphene is mechanically exfoliated into solvents where the
37 graphene – liquid interfacial energy is equivalent to the cohesive inter-layer energy of
38 graphite sheets.⁹⁻¹¹ However, unless the graphene is chemically modified to graphene oxide
39 (which alters the electronic properties of the sheet; graphene oxide is an insulator)
40 aggregation and settling occurs over time.

41 Ionic liquids (ILs) – pure salts that melt below 100 °C^{12,13} – have many useful physical
42 properties which may be tuned by varying the structure of the cation or anion.^{12,14,15} The
43 inherently high conductivity of ILs makes them attractive for graphene-based technologies.
44 Graphene has been mechanically exfoliated into ILs to successfully produce suspensions
45 reported to be stable for up to three weeks. In this work we show that graphene can be
46 spontaneously exfoliated at room temperature when graphite is immersed in certain ILs. By
47 investigating the interaction of highly ordered pyrolytic graphite (HOPG) with seven
48 different ionic liquids at the nanoscale, we identify the molecular mechanisms that confer
49 some ILs their exfoliating properties. The full names, abbreviations, and physical properties
50 of the ILs investigated in this work are summarised in Table 1. Four of these, EMIm Ac,

51 EMIm TFMS, BMIm BF₄ and BMIm SCN, have surface tension values within the
52 ‘goldilocks’ 40 - 50 mN/m range reported to stabilise exfoliated graphene.¹⁶ 3 ml of each IL
53 was added to 0.1 g of ground HOPG in separate sample vials *without mixing, stirring or*
54 *sonicating* and the appearance of the resulting liquid monitored over time at 22 °C.
55 Discoloration progressively developed in EMIm Ac and EMIm TFMS and the solid
56 fragments of HOPG disappeared, while the appearance of the other samples did not change.
57 Comparison between the appearance of pure and graphene-loaded EMIm Ac and EMIm
58 TFMS is shown in Fig. 1. Tyndall effect scattering was noted upon shining a laser through
59 the EMIm Ac and EMIm TFMS samples, and Raman spectroscopy confirmed the presence of
60 graphene sheets comprising only a few layers (see Supplementary Fig. 1). For both graphene-
61 loaded IL samples, the Raman spectra revealed characteristic graphene peaks.¹⁷
62 Deconvolution of the G’ (2D) band (see Supplementary Fig. 2) reveals four and three
63 distinctly superimposed bands for EMIm Ac and EMIm TFMS, respectively, which are the
64 fingerprint of few-layer graphene.

65 To probe the spontaneous exfoliation process directly and in real-time, the surface evolution
66 of HOPG fully immersed in each IL was imaged *in-situ* by time-lapse amplitude-modulated
67 atomic force microscopy (AM-AFM). The whole exfoliation process can be followed in time
68 lapse movies created from 2 μm × 2 μm images of the HOPG surface. Over time the
69 appearance of the HOPG undergoes dramatic changes, but only in the presence of EMIm Ac
70 and EMIm TFMS (Supplementary Movies 1 and 2 respectively); No changes were seen for
71 the other ILs. Figure 1 presents some of the critical steps of the exfoliation process seen by
72 AFM. At 4 minutes after immersion (Fig. 1 a), the planes and step edges characteristic of
73 intact HOPG surfaces¹⁸ are visible. After 137 mins for EMIm Ac and 37 mins for EMIm
74 TFMS, distinct changes are visible (Fig. 1b) with the HOPG surface roughening, particularly
75 in the areas around the step edges.



76

77 **Figure 1.** $2\ \mu\text{m} \times 2\ \mu\text{m}$ AM-AFM phase images of the EMIm Ac (a, b and c) - and EMIm TFMS (f, g and h) -
 78 HOPG interface. IL immersion times are given at the top of each image (see Supplementary Movies 1 and 2 for
 79 a full time-lapse evolution). The blue arrows point to areas of the HOPG surface which appear to erode over
 80 time. Figure d and i show vials of the pure EMIm Ac and EMIm TFMS, respectively, and the ILs + 0.1 g HOPG
 81 sample left untouched at room temperature for ~ 2 weeks. Figure e and j reveal the Tyndall effect for the IL +
 82 HOPG solutions indicating a very fine suspension in the IL.

83

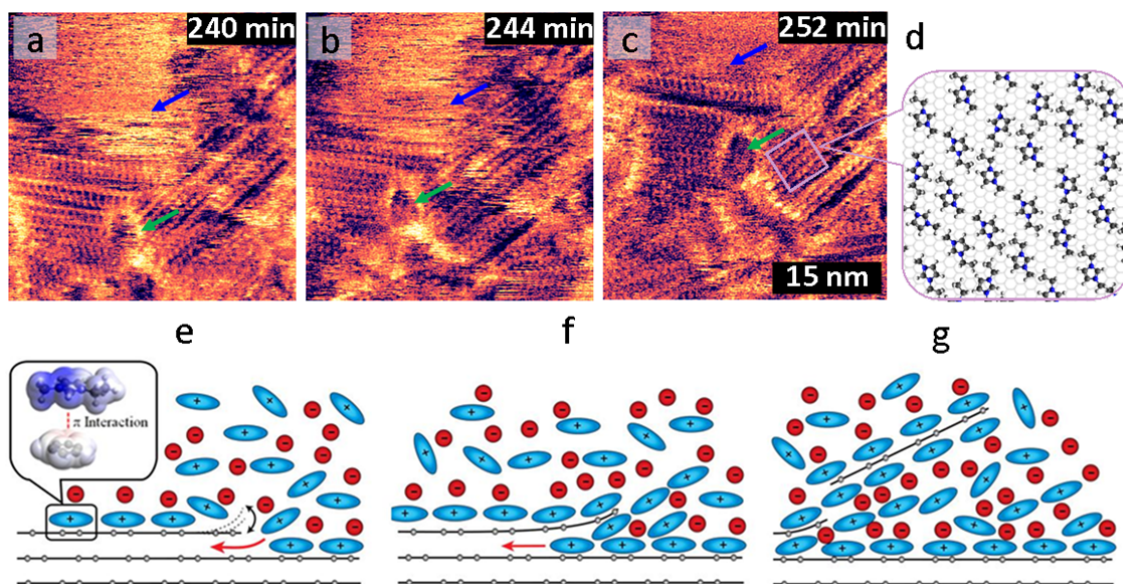
84 In places (see blue arrows in Fig. 1), step edges grow significantly wider, indicating erosion
 85 of the surface. The effect is most notable for EMIm TFMS. After 190 mins for EMIm Ac and
 86 72 mins for EMIm TFMS the HOPG surface bears little resemblance to the original HOPG.
 87 The flat terraces observed initially are absent, and replaced by amorphous domains separated
 88 only by the most pronounced step edges. The appearance of the surface at longer time periods
 89 was similar, consistent with continued exfoliation. Imaging of surface locations not
 90 previously imaged by the tip showed similar features at all times (c.f. Supplementary Figure
 91 3), ruling out the possibility of tip-induced effects.

92 In order to gain further insights into the molecular mechanisms inducing exfoliation of the
 93 HOPG, molecular-resolution time lapse-movies were acquired (Supplementary Movie 3).
 94 Selected nanoscale images of the process are shown in Fig. 2a-c for EMIm - Ac together
 95 with the identified mechanism (Fig. 2e-g). Rows of ellipses cover most of the surface,

96 arranged according to a hexagonal symmetry templated by the underlying HOPG. In a
97 previous study¹⁹ of the EMIm TFSI – HOPG interface (where graphene exfoliation is not
98 observed, c.f. Table 1) we determined that these ellipses show individual EMIm⁺ ions
99 adsorbed onto the HOPG. Distinct features due to TFSI adsorption were also present. Here,
100 the surface rows for EMIm Ac visible in Fig. 2a-c all have the same appearance, indicating
101 that the anions are excluded from the surface layer. This is reasonable since both Ac⁻ and
102 TFMS⁻ are substantially more hydrophilic than TFSI⁻, and will hence be less strongly
103 attracted to the HOPG surface. (At the same magnification the appearance of EMIm TFMS –
104 HOPG interface is similar to EMIm Ac). The featureless area at the top left (blue arrow) is a
105 graphene flake already (or partially) detached from the surface. Ion positions cannot be
106 resolved because the mobility of the flake. Over time, the flake moves towards the top of the
107 image, exposing new cation rows running in two main directions around a central defect
108 (green arrow). At 240 mins, the step edge on the right hand side of the defect is white,
109 indicating strong interactions between this area and the AFM tip. As simulations²⁰ and
110 experiments^{19,20} have shown that ILs of this type do not chemically react with graphene or
111 HOPG, these strong interactions can only be due to the step edges peeling away from the
112 underlying sheet. At 244 mins and 252 mins, both sides of the defect appear lighter, and the
113 defect has grown wider as the graphene on either side of the defect pulls apart. Over time,
114 these flakes detach from the surface.

115 The two ionic liquids have surface tensions in the so-called ‘goldilocks’ zone for stabilizing
116 graphene, meaning that the interfacial energy between the IL and a graphene sheet is
117 comparable to that for two sheets in contact. This energy matching, the ability of the
118 imidazolium cations to pi-stack onto HOPG, and the high ionic concentration drives cations
119 to intercalate between graphene sheets via step edges.

120



121

122 **Figure 2.** (a - c) 40 nm × 40 nm phase images of the EMIm Ac - HOPG interface obtained sequentially (time
 123 indicated as an inset to the image). The cantilever was kept in a single imaging location during imaging,
 124 meaning that the observed features are a consequence of changes to the HOPG surface. Coloured arrows mark
 125 the surface locations which appear to peel away from the surface. d) Schematic of the lateral arrangement of
 126 adsorbed EMIm⁺ cations at the HOPG interface. (e - g) Schematic of the exfoliation mechanism which occurs
 127 spontaneously in the presence of EMIm Ac and EMIm TFMS.
 128
 129

130 Although BMIm BF₄ and BMIm SCN meet the surface tension criterion, the absence of
 131 spontaneous exfoliation suggests additional requirements. If we assume that the time required
 132 for cation intercalation is determined by the cations ability to penetrate at step edges as they
 133 fluctuate (peel away from and re-bind to the underlying sheet, indicated by the black arrow
 134 in Fig. 2b) due to thermal motion, steric interactions between step edges and the C₄ alkyl
 135 chain of BMIm BF₄ and BMIm SCN would prevent intercalation. Consistently, the time to
 136 exfoliation is lower for EMIm TFMS than EMIm Ac at every temperature due to lower
 137 viscosity of EMIm TFMS. Lower viscosity thermally-induced step edge oscillations are
 138 larger, allowing cations to more readily move between sheets at step edges as gateways
 139 develops. In this model, intercalation is a co-operative process; once the first cation inserts
 140 under the step edge, the energy barrier to the next cation is reduced – the first cation holds the

141 gateway open – and the process cascades. IL ions spread between graphene sheets until an
142 imperfection is reached, at which point the sheet breaks away and is exfoliated into solution.

143 The proposed molecular model hinges on thermal fluctuations naturally occurring at step
144 edges of the HOPG. In order to verify this hypothesis, we investigated the effect of
145 temperature using AFM between 25°C and 80°C. Freshly cleaved HOPG surfaces were
146 immersed in each IL at different temperatures and the exfoliation process followed in real
147 time. Increasing the temperature dramatically decreased the time to exfoliation (see
148 Supplementary Fig. 4), indicating an Arrhenius-type process in support of our hypothesis.
149 The measured activation energies of 39 kJ/mol and 27 kJ/mol for EMIm Ac and EMIm
150 TFMS, respectively, are comparable with calculated adsorption energies for benzene (19
151 kJ/mol) and pyrene (43 kJ/mol) to graphene,²¹ and thus consistent with the proposed
152 mechanism of dissociation of pi-stacked step edge rings from the HOPG layer below.

153 In summary, we have shown that EMIm TFMS and EMIm Ac spontaneously exfoliate
154 graphene from HOPG due to matched IL – graphene and graphene – graphene interfacial
155 energies, the formation of an EMIm⁺-rich layer on HOPG, and the fact that EMIm⁺ cations
156 are small enough to intercalate between graphene sheets via step edges. Our results pave the
157 way for the design and development of other liquids and solutions allowing spontaneous
158 graphene exfoliation, and enable graphene production and stable storage on large scales.

159

160 **Acknowledgements**

161 R.A. thanks the Australian Research Council Future Fellowship (FT120100313). This
162 research was supported by an Australian Research Council Discovery Project
163 (DP120102708) and Equipment Grant (LE110100235).

164 **Supplementary Information** is linked to the online version of the paper at
165 www.nature.com/nature.

166 **Author contributions**

167 A.E. and R.A. conceived the project. A.E. performed the AFM measurements with guidance
168 from K.V.. B.M. performed the Raman measurements. A.E. and B.M. performed the surface
169 tension measurements. R.A. wrote the manuscript. All authors participated in research
170 discussions.

171 **References**

- 172 1 Du, W., Jiang, X. & Zhu, L. From graphite to graphene: direct liquid-phase
173 exfoliation of graphite to produce single- and few-layered pristine graphene. *Journal*
174 *of Materials Chemistry A* **1**, 10592-10606 (2013).
- 175 2 Lu, W. *et al.* High-yield, large-scale production of few-layer graphene flakes within
176 seconds: using chlorosulfonic acid and H₂O₂ as exfoliating agents. *J. Mater. Chem.*
177 **22**, 8775-8777 (2012).
- 178 3 Behabtu, N. *et al.* Spontaneous high-concentration dispersions and liquid crystals of
179 graphene. *Nat Nano* **5**, 406-411 (2010).
- 180 4 Novoselov, K. S. *et al.* Electric Field Effect in Atomically Thin Carbon Films.
181 *Science* **306**, 666-669 (2004).
- 182 5 Allen, M. J., Tung, V. C. & Kaner, R. B. Honeycomb Carbon: A Review of
183 Graphene. *Chem. Rev.* **110**, 132-145 (2010).
- 184 6 Subrahmanyam, K. S., Vivekchand, S. R. C., Govindaraj, A. & Rao, C. N. R. A study
185 of graphenes prepared by different methods: characterization, properties and
186 solubilization. *J. Mater. Chem.* **18**, 1517-1523 (2008).
- 187 7 Soldano, C., Mahmood, A. & Dujardin, E. Production, properties and potential of
188 graphene. *Carbon* **48**, 2127-2150 (2010).
- 189 8 Choi, W., Lahiri, I., Seelaboyina, R. & Kang, Y. S. Synthesis of Graphene and Its
190 Applications: A Review. *Crit. Rev. Solid State Mat. Sci.* **35**, 52-71 (2010).
- 191 9 Lu, J. *et al.* One-Pot Synthesis of Fluorescent Carbon Nanoribbons, Nanoparticles,
192 and Graphene by the Exfoliation of Graphite in Ionic Liquids. *ACS Nano* **3**, 2367-
193 2375 (2009).
- 194 10 Wang, X. *et al.* Direct exfoliation of natural graphite into micrometre size few layers
195 graphene sheets using ionic liquids. *Chem. Commun.* **46**, 4487-4489 (2010).
- 196 11 Nuvoli, D. *et al.* High concentration few-layer graphene sheets obtained by liquid
197 phase exfoliation of graphite in ionic liquid. *J. Mater. Chem.* **21**, 3428-3431 (2011).
- 198 12 Welton, T. Room-Temperature Ionic Liquids. Solvents for Synthesis and Catalysis.
199 *Chem. Rev.* **99**, 2071-2083 (1999).
- 200 13 Wilkes, J. S. A Short History of Ionic Liquids - from Molten Salts to Neoteric
201 Solvents. *Green Chem.* **4**, 73-80 (2002).
- 202 14 Endres, F. *et al.* in *Ionic Liquids Uncoiled* 1-27 (John Wiley & Sons, Inc., 2012).

- 203 15 Hayes, R., Warr, G. G. & Atkin, R. Structure and Nanostructure in Ionic Liquids.
204 *Chem. Rev.* **115**, 6357-6426 (2015).
- 205 16 Hernandez, Y. *et al.* High-yield production of graphene by liquid-phase exfoliation of
206 graphite. *Nat Nano* **3**, 563-568 (2008).
- 207 17 Ferrari, A. C. *et al.* Raman Spectrum of Graphene and Graphene Layers. *Phys. Rev.*
208 *Lett.* **97**, 187401 (2006).
- 209 18 Albrecht, T. R. & Quate, C. F. Atomic resolution imaging of a nonconductor by
210 atomic force microscopy. *Journal of Applied Physics* **62**, 2599-2602 (1987).
- 211 19 Elbourne, A. *et al.* Nanostructure of the Ionic Liquid–Graphite Stern Layer. *ACS*
212 *Nano* **9**, 7608-7620 (2015).
- 213 20 Page, A. J. *et al.* 3-Dimensional Atomic Scale Structure of the Ionic Liquid–Graphite
214 Interface Elucidated by AM-AFM and Quantum Chemical Simulations. *Nanoscale* **6**,
215 8100-8106 (2014).
- 216 21 Tournus, F., Latil, S., Heggie, M. I. & Charlier, J. C. π -stacking interaction between
217 carbon nanotubes and organic molecules. *Phys. Rev. B.* **72**, 075431 (2005).
- 218 22 Ravula, S., Baker, S. N., Kamath, G. & Baker, G. A. Ionic liquid-assisted exfoliation
219 and dispersion: stripping graphene and its two-dimensional layered inorganic
220 counterparts of their inhibitions. *Nanoscale* **7**, 4338-4353 (2015).
- 221 23 Kim, J., Kim, F. & Huang, J. Seeing graphene-based sheets. *Materials Today* **13**, 28-
222 38 (2010).
- 223 24 Voitchovsky, K., Kuna, J. J., Contera, S. A., Tosatti, E. & Stellacci, F. Direct
224 Mapping of the Solid-Liquid Adhesion Energy with Subnanometre Resolution. *Nat*
225 *Nano* **5**, 401-405 (2010).
- 226 25 Voitchovsky, K. & Ricci, M. in *Conference on Colloidal Nanocrystals for Biomedical*
227 *Applications VII* Vol. 8232 *Proceedings of SPIE* (Spie-Int Soc Optical Engineering,
228 Po Box 10, Bellingham, Wa 98227-0010 Usa, San Francisco, CA, 2012).

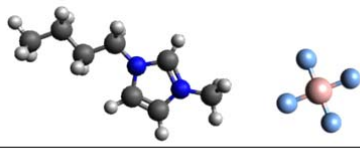
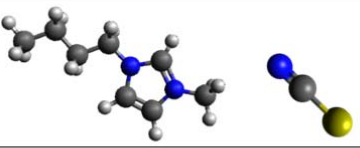
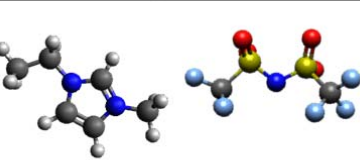
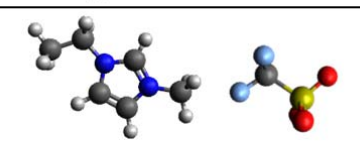
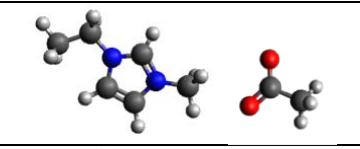
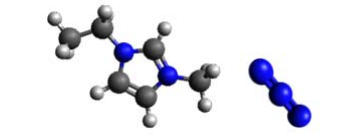
229

230

231

232 **TABLES**

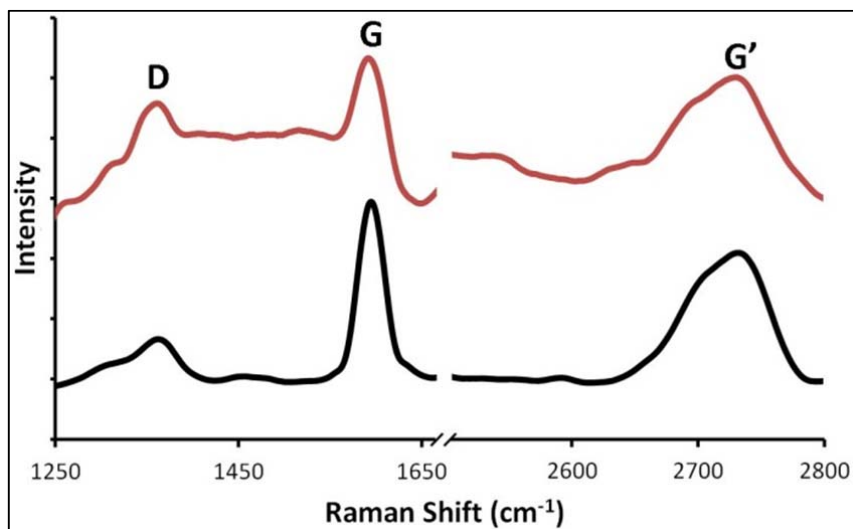
233 **Table 1.** Name, abbreviation (Abbrev.), ionic structure and surface tension value (mN/m) of the 6 ILs
 234 investigated. In the structural models carbon atoms are grey, nitrogen are blue, oxygen are red, hydrogens are
 235 white, sulphur is yellow, and fluorine is light blue.

| Name | Abbrev. | Structure | Surface Tension (mN/m) |
|---|----------------------|--|------------------------|
| 1-Butyl-3-methylimidazolium tetrafluoroborate | BMIm BF ₄ |  | 43.7 |
| 1-Butyl-3-methylimidazolium thiocyanate | BMIm SCN |  | 47.1 |
| 1-ethyl-3-methylimidazolium bis(trifluoromethylsulfonyl)imide | EMIm TFSI |  | 33.9 |
| 1-ethyl-3-methylimidazolium trifluoromethanesulfonate | EMIm TFMS |  | 42.1 |
| 1-ethyl-3-methylimidazolium Acetate | EMIm Ac |  | 42.5 |
| 1-ethyl-3-methylimidazolium Dicyanamide | EMIm DCA |  | 56.7 |

236

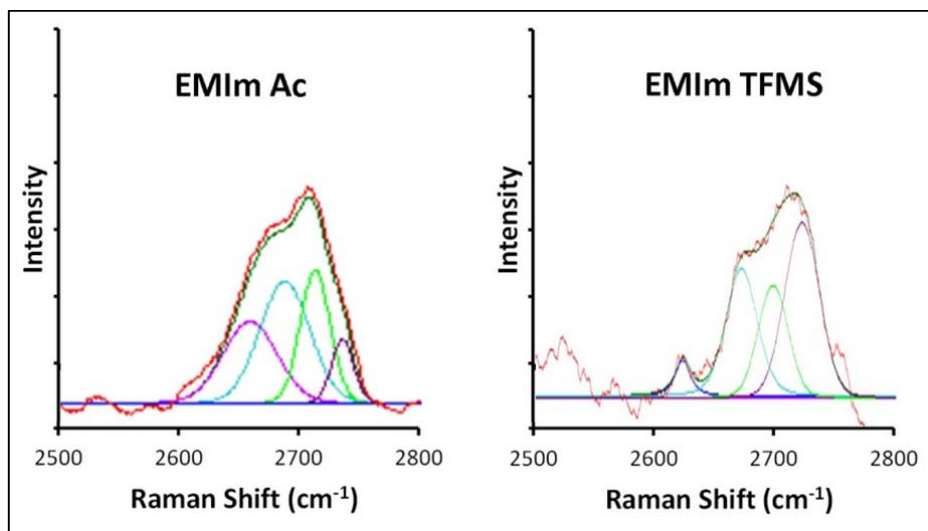
237

238



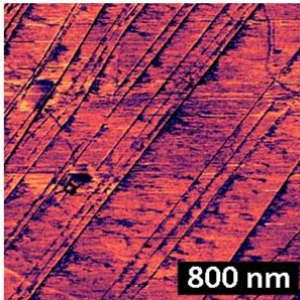
240

241 **Supplementary Figure 1.** Raman spectra of graphene flakes obtained from the ILs EMIm Ac (black line) and
 242 EMIm TFMS (red line). The three distinct regions of graphene samples are labeled in the spectra. The peaks are
 243 characteristic of graphene: D band at ~ 1350 cm⁻¹, the G band at ~ 1580 cm⁻¹ and the G' (2D) band at ~ 2720 cm⁻¹.
 244 The I_G/I_D ratio (~ 6 for EMIm Ac and ~ 2 for EMIm TFMS) is consistent with values reported previously for
 245 high-quality graphene produced via exfoliation.^{9,10,22} Deconvolution of the G' (2D) band (see Supplementary
 246 Fig. 2) reveals four and three distinctly superimposed bands for EMIm Ac and EMIm TFMS, respectively,
 247 which are the fingerprint of few-layer graphene; pure HOPG exhibits two sharp peaks upon G' band
 248 deconvolution, which allows graphene and HOPG to be easily distinguished.^{17,23}
 249



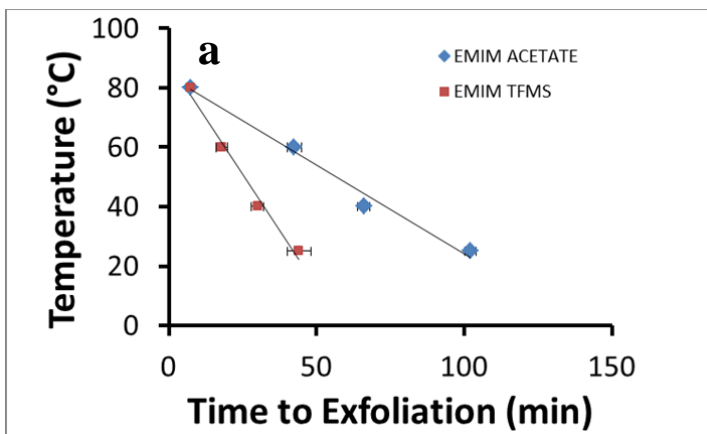
250

251 **Supplementary Figure 2.** G' band deconvolution for graphene samples obtained from EMIm Ac and EMIm
 252 TFMS revealing four and three distinctly superimposed bands, respectively.

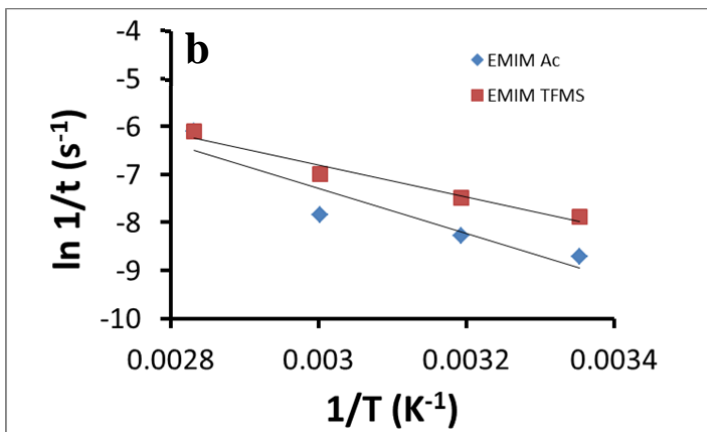


253

254 **Supplementary Figure 3.** $2\ \mu\text{m} \times 2\ \mu\text{m}$ AM-AFM phase image of the EMIm TFMS - HOPG interface obtained
 255 at a previously un-imaged surface location. The image shows similar surface degradation to that of Figure 2,
 256 establishing that the exfoliation is happening spontaneously at a global scale.



257



258

259

260 **Supplementary Figure 5. A)** Plot of exfoliation time (mins) vs. system temperature (°C) for the EMIm Ac –
 261 and EMIm TFMS – HOPG systems, and **B)** Arrhenius plot of $1/T$ vs. $\ln 1/t$ (sec) for the exfoliation of graphene
 262 in EMIM Ac and EMIM TFMS. The t measurement denotes the time at which exfoliation was first noted during
 263 an AM-AFM experiment and T indicates the temperature of the corresponding experiment. The calculated
 264 activation energy for exfoliation in EMIM Ac and EMIM TFMS is 38.7 kJ/mol and 27.5 kJ/mol, respectively. A
 265 distinct increase of the spontaneously exfoliation rate is noted with increased temperature for both systems.

266

267

268 **Methods and Materials**

269 ***Consumables***

270 EMIm TFSI, EMIm TFMS, EMIm DCNA, and EMIm Ac were purchased from Io-Li-Tec,
271 Ionic Liquids Technologies (Germany) in the highest purity available (>99.9%). Highly
272 ordered pyrolytic graphite (HOPG) surfaces were bought from NT-MDT Co., Russia, and
273 cleaved along the basal plane using adhesive tape immediately prior to the experiment. The
274 HOPG was therefore atomically smooth and clean.

275 ***AFM Measurements***

276 The systems were studied using an Asylum Research Cypher Atomic Force Microscope
277 (Cypher AFM) at room temperature (25°C). Images were obtained using ArrowUHFauD
278 (NanoWorld, Switzerland, nominal spring constant $k_c = 6 \text{ N m}^{-1}$). Each cantilever was
279 calibrated using by the thermal spectrum method in IL prior to use, producing a well-defined
280 resonance peak, and the lever sensitivity was determined using force spectroscopy. Cantilever
281 tips were irradiated with UV light for 15 minutes prior to experiment to remove organic
282 contaminants. Experiments were completed in a droplet exposed to the atmosphere within the
283 AFM box (a sealed enclosure). As the ILs are hygroscopic, the water content of the liquid
284 increases over the course of an experiment. Karl Fischer titration water content of IL
285 collected from the cell after an experiment had a value of no more than ~1 wt% which
286 depended slightly on the ambient humidity. To eliminate the possibility that water contributes
287 to the observed graphene exfoliation additional experiments were performed with IL pre-
288 doped with 2 wt% water, a concentration twice that of the typical recovered IL. These
289 experiments showed no increase in exfoliation time, meaning that water is not a contributing
290 factor to the exfoliation mechanism. The features of all images presented rotated as the scan

291 angle was changed and scaled correctly with scan size, confirming they are not imaging
292 artefacts. All dimensions provided are ± 0.01 nm unless stated otherwise.

293 During an AM-AFM experiment an oscillating cantilever tip scans the surface to create
294 interfacial images; the tip-sample distance (z-piezo) is continually adjusted to maintain a
295 user-set oscillation amplitude as the tip encounters adsorbed material. In this way, interfacial
296 images are generated by the variation in the z-piezo position and cantilever's phase which are
297 both a consequence of the adsorbate's relative stiffness. Hence, in an AM-AFM image the
298 light areas indicate relatively immobilised material between the tip, while the dark areas
299 indicate the position of more compliant matter.²⁴ However, it must be noted that this is a
300 simplified definition provided for interpretation, while the precise tip-sample dynamics are
301 much more complex.^{24,25} During imaging, the working amplitude/free amplitude values
302 (A/A_0) of ≥ 0.7 were typically used with the free liquid amplitude (A_0) of the cantilever ≈ 1
303 nm for nanoscale image and ≈ 5 nm for large scale images. At the nanoscale these parameters
304 mean that the phase and amplitude vary in response to the liquid compliance between the tip
305 and the surface, meaning the AFM directly probes the adsorbed layer ions without
306 significantly interacting with the HOPG surface. For larger images the larger oscillation
307 amplitude allows IL ions to be "squeezed out" from between the cantilever and the surface,
308 meaning the HOPG is directly probed. It should be noted that the Stern layers in all systems
309 are dynamic, with constant diffusion of ions in and out of the structures. The AM-AFM
310 captures the average structure over the course of producing an image (~ 4 minutes).

311 ***Raman Spectroscopy***

312 Solutions of IL and HOPG were obtained through simple addition of graphitic flakes cleaved
313 from an HOPG substrate to the IL and leaving them sealed for several weeks. Spectra were
314 obtained by placing a drop of the sample onto stainless steel, The spectrum in pure IL served

315 as a baseline and was subtracted from the spectrum of graphene-loaded IL. Raman spectra
316 were obtained at 20 °C using an inVia Renishaw Raman spectrometer at 514 nm with edge
317 filters. Laser incident power was measured to be 0.125 mW. Spectra were acquired by
318 averaging 5 acquisitions of 10 seconds with a 50x objective. These conditions resulted in no
319 spectral changes over time and no visual degradation, or modification of the sample under the
320 microscope.

321 *Surface Tension Measurements*

322 IL surface tension values were determined using the pendant drop method (air in IL) with an
323 OCA20 measuring instrument (DataPhysics, Germany). 20 mLs of each IL was placed in a
324 sealed vessel, and a stable air bubble was produced from the pendant drop needle. The
325 instrument software package was then used to fit the Young-Laplace equation to the pendant
326 drop profiles, allowing the calculation of the IL-air interfacial surface tension.